한국소음진동공학회 1995년도 추계학술대회논문집 pp.7-15

APPLICATION OF SOUND INTENSITY METHOD TO NOISE CONTROL ENGINEERING AND BUILDING ACOUSTICS

Hideki Tachibana

Institute of Industrial Science, University of Tokyo
Roppongi 7-22-1, Minato-ku, Tokyo, 106 Japan

1. INTRODUCTION

Sound pressure and particle velocity are the most essential quantities prescribing a sound field; they correspond to voltage and electric current respectively, in electric system. As electric power is the product of voltage and electric current, sound intensity is the product of sound pressure and particle velocity and it means the acoustic power passing through a unit area in a sound field. Although the definition of sound intensity is very simple as mentioned above, the method of measuring this quantity has not been realized for a long time, because it has been very difficult to measure the particle velocity simultaneously with the sound pressure. Owing to the recent development of such technologies as transducer production and digital signal processing, it has finally been realized [1]. According to the sound intensity (SI) method, the sound power flow in an arbitrary sound field can be directly measured as a vector quantity. In this paper, the principle of the SI method is briefly explained at first and some examples of its application made in the author's laboratory are introduced.

2. MEASUREMENT PRINCIPLE

Sound intensity is defined as,

$$\bar{I} = \overline{p(t) \cdot \bar{u}(t)} \qquad (1)$$

where $p(t)$ is sound pressure, $\bar{u}(t)$ is particle velocity and — denotes time averaging.

In the sound field consisting of only a plane wave, there exists the following relationship between sound pressure and particle velocity.

$$u(t) = p(t) / \rho c \qquad (2)$$

where ρ is the density of air and c is the sound velocity. In this case, the absolute value of the sound intensity can be obtained only from the sound pressure as follows.

$$I = \overline{p^2(t)} / \rho c \qquad (3)$$

However, Eq.(2) is not necessarily valid for general sound fields and sound intensity must be obtained according to Eq.(1). On this point, the measurement of particle velocity is a serious problem. It is much difficult to measure the particle velocity with correct phase relationship with the sound pressure and this fact has prevented the realization of the sound intensity measurement for a long time.

Regarding this problem, T. Schultz invented an epoch-making idea called "2-microphone method" in 1956 [1]. In this method, the second term of Eq.(4) is approximated by the finite difference between the sound pressures at closely spaced two points as expressed by Eq.(5) and consequently the particle velocity is approximated by Eq.(6).

$$\rho \frac{\partial u_r}{\partial t} + \frac{\partial p}{\partial r} = 0 \qquad (4)$$

$$\frac{\partial p}{\partial r} \approx \frac{p_2(t) - p_1(t)}{\Delta r} \qquad (5)$$

$$u_r(t) \approx -\frac{1}{\rho \Delta r} \int_{-\infty}^{t} \left[p_2(\tau) - p_1(\tau) \right] d\tau \qquad (6)$$

where $p_1(t)$ and $p_2(t)$ are the sound pressures at the two points and Δr is the separation distance between them. Consequently, the sound intensity component in the direction of r can be approximated

as follows.

$$I_r \approx -\frac{1}{\rho \Delta r} \overline{\frac{p_1(t)+p_2(t)}{2} \int_{-\infty}^{t} [p_2(\tau)-p_1(\tau)]\, d\tau} \qquad (7)$$

Figure 1(a) shows the actual measurement system based on the principle mentioned above. This method is called "direct method". In this case, the two channels must have the identical performances in both of amplitude and phase characteristics for all of the components such as the pressure microphones, amplifiers and band pass filters. This point has been the most serious problem in the sound intensity measurement. Fortunately, it has been almost solved by the recent developments of transducer manufacturing and digital signal processing technologies.

By expressing Eq.(7) in the frequency domain, we have,

$$I_r(f_1, f_2) \approx -\frac{1}{2\pi\rho\Delta r} \int_{f_1}^{f_2} \frac{\mathrm{Im}\{G_{12}(f)\}}{f} df \qquad (8)$$

where $\mathrm{Im}\{G_{12}(f)\}$ is the imaginary part of the cross-spectrum density function between $p_1(t)$ and $p_2(t)$. The calculation according to this formula can be easily realized by use of FFT analyzer as shown in Fig.1(b). This method is called "cross-spectrum method" or "FFT method".

As an sound intensity probe, two pressure-type condenser microphones with identical amplitude and phase characteristics are used in side by side or face to face configurations as shown in Fig.2.

3. APPLICATIONS

3.1 Sound Radiation Measurement

(1) Sound radiation from a vibrating plate [2)]

As a basic study, the sound intensity radiation from a vibrating strip of vinyl chloride plate was measured. As shown in Fig.3, it was excited at the center point and the sound intensity in the near field and the vibration velocity on the plate were measured. In these results, we can see that the "source" positions from which the sound is radiated and the "sink" positions into which the sound is absorbed are arrayed alternately.

(2) Sound radiation from a violoncello [3)]

Musical instruments are much interesting subjects of acoustics and a lot of investigations have been made. We have measured the sound power radiation characteristics of various musical instruments by the SI method. Among them, the sound intensity radiation patterns from a violoncello are shown here. In this measurement, the second string (d, open) was played by a bow which was automatically moved by using a reversible motor and the sound intensity distributions were obtained in each 1/3 octave band. As a result, Fig. 4 shows the sound intensity vector maps measured in two sections perpendicular to the sound board through the f-hole. In the case of 160 Hz band in which the fundamental tone of 147 Hz is included (a), the sound radiation pattern is uniform. On the other hand, in the case of 315 Hz band (b), it should be noted that sound power is absorbed in the lower part of the body.

(3) Sound radiation from building structure elements [4)]

Building structures can radiate sound when they vibrate. As a model experiment regarding this kind of problem, an I-shaped steel beam of a section of 120 mm x 60 mm and 1 m long was hung in an anechoic room and the sound intensity around it was measured by exciting an end of the beam. In this experiment, the measurement was conducted in both cases of with and without vibration damping treatment on the web of the beam. In Fig.5 (a) and (b), the solid lines indicate the sound intensity vectors measured by stationary random excitation and the dotted lines indicate those measured by impulsive excitation. Each vector was obtained from the sound intensities measured in x and y directions. Almost all results measured by the two ways of excitation are in good agreement in both cases of with and without damping treatment. From these results, the radiated sound power per unit length of the beam was calculated by integrating the sound intensity component normal to the measurement line. Figure 6 shows the efficiency of the vibration damping treatment which was obtained as the difference of the sound power between the cases of without and with damping treatment.

(4) Sound radiation from rotating automobile tires [5]

In order to investigate the sound radiation characteristics of rolling automobile tires, a field experiment was performed by applying the SI method. In this experiment, a trailer equipped with a probe scanning machine was driven on a test course and the normal intensity distribution on the plane of 1 m x 1 m area which was set parallel to the rear tire was measured in actual running condition. Figure 7 (a) shows the measured results for a rib tire, in which we can see that the front and rear parts of the contact patch are the dominant sound sources. Figure 7 (b) shows that for a lug tire, in which we can see that the contact patch is the main sound source and the sound radiation pattern is much more complicated than the case of the rib tire.

(5) Sound radiation from road vehicles and train [6,7]

For the prediction and reduction of traffic noises, it is important to know the sound radiation characteristics of noise sources. As an investigation for this purpose, the sound radiation from actually running road vehicles were measured using the SI method [6]. The measurement was performed on a well-conditioned test course by setting a 3-dimensional intensity probe at a point 3.3 m apart from the center line of the running path, by changing the height of the probe. Figure 8 (a) and (b) shows the measured results for a 2000 cc passenger car and a 10 ton heavy truck, respectively. In these figures, the solid lines are the measured intensities and their extensions are indicated by the dotted lines. As shown in (a), in the case of the passenger car, it can be seen that the extended lines of the vectors concentrate at the contact patch of the tires. It might indicate that the tire/road noise is dominant. On the other hand, in the case of the heavy truck shown in (b), the lines seems to concentrate at the point just under the body. This results might indicate that the engine noise is dominant under the condition of 40 km/h running speed for heavy trucks.

In the same way, the sound radiation from a Japanese super express train Shinkansen was measured [7]. In this case, a vertical array composed of eight 2-dimensional probes was set aside the rail on an elevated construction. Figure 9 show the intensity vectors averaged for a train passage measured under the condition of without barrier (a) and after the construction of a reflective barrier (b). In the former case, the extended lines of the vectors seem to concentrate at the lower part of the train. This might mean that the wheel rolling noise is dominated. In the latter case, the shielding effect of the barrier is clearly seen and the extended lines of the vectors go toward the higher position. This might be attributed to multiple reflection between the body and the barrier.

3.2 Sound Field Analysis

(1) The effect of sound diffusers [8]

In auditoria, walls are often made irregular-shaped to make the sound field diffusive. As an experimental study to investigate the effect of such acoustic treatments, the sound reflection by a plane with a triangular projection and that with a semi-circular projection were measured by the SI method. Figure 10 (a) shows the sound intensity flow of 500 Hz over the two reflecting planes. In this case, the wave length is larger than the scale of the section of the projections and the sound intensity reflection patterns are almost the same. In both cases, sound intensity vortices are seen. On the other hand, Figure 10 (b) shows the sound intensity flow of 8 kHz. In this case, the wavelength is smaller than the scale of the projections and the two reflection patterns are much different. These results indicate that the effect of sound diffusion is different in high frequencies between the two types of projections.

(2) Sound diffraction over an active noise barrier [9]

In order to examine the effect of "active noise barrier", a scale model experiment was carried out using feedforward adaptive control ANC technique. Figure 11 shows an example of the experimental result of sound intensity vectors over the barrier without ANC (a) and with ANC (b). It can be seen that the diffracted sound is much weakened behind the barrier by applying ANC and the secondary source seems to absorb the sound energy in this case.

(4) Sound propagation in a maze-type duct [10]

ANC are being applied to HVAC duct systems to increase the noise reduction in low frequencies. In order to examine the effect of ANC when applied to a multiple chamber (maze-type) duct, scale model experiment and numerical analysis were carried out [10]. Figure 12 shows the result of the scale model experiment (a) and that of the FEM calculation (b). In these results, we can see that the intensity flow obtained by the experiment and that by the calculation are quite similar both in the cases of ANC ON and OFF and that the sound transmission to the outlet is much decreased by ANC.

(5) Measurement of sound diffusiveness in rooms [11]

As a trial to observe the extent of acoustic diffusiveness in a room, the 3-dimensional sound intensity measurement using an impulsive sound source was applied in various rooms. Among the results, Fig.13 shows the vector loci of instantaneous sound intensity on the horizontal (x-y) plane measured in a concert hall (a) and in a reverberation room (b). In the former case, the direct sound from the sound source (x-direction) and discrete early reflections from right and left directions are clearly seen. On the other hand, in the latter case, the reflections after the direct sound are omnidirectional; it indicates that the sound field is much diffusive.

3.3 Sound Insulation Measurement [12]

The SI method can be effectively applied to sound insulation measurement. As an example, Fig.14 shows the measured results of sound power flow transmitting through a window. In this measurement, the sound source was located inside the room and the sound intensity normal to the window was measured outside at a lot of discrete points. In these results, we can see that sound power uniformly transmits through the window in the case of low frequency (250 Hz) as shown in (a), whereas sound power transmits dominantly through the edge parts of the window in the case of high frequency (2 kHz) as shown in (b). As is clearly seen in this example, the SI method is very effective for the detection of acoustic weak points in sound insulation of building walls.

4. CONCLUSIONS

In this paper, some examples of acoustic radiation, propagation and transmission measurements made by the SI method have been introduced. According to the SI method, sound pressure and particle velocity can be measured simultaneously and almost all acoustic quantities can be obtained. Therefore, this acoustic measurement method will be much more widely applied in the future.

REFERENCES

1) F.J.Fahy : Sound Intensity, Elsevier Applied Science Publishers, 1989
2) Y.Hidaka, S.Ankyu and H.Tachibana : Sound field analyses by complex sound intensity, J. Acoust. Soc. Jpn.(J), Vol.43 No.12, pp.994-1000, 1987
3) H.Tachibana and Y.Hidaka : Visualization of sound radiation from a violoncello, J.Acoust.Soc.Jpn.(J), Vol.46 No.10, pp.864-866, 1991
4) H.Yano, Y.Hidaka and H.Tachibana : Sound and vibration measurements by impulsive excitation, J. Acoust. Soc. Jpn.(E), Vol.11 No.2, pp.77-82, 1990
5) Y.Oshino and H.Tachibana : Noise source identification of rolling tires by sound intensity measurement, J. Acoust. Soc. Jpn.(E), Vol.12 No.2, pp.87-92, 1991
6) H.Tachibna and Y.Oshino : Sound intensity radiation patterns of actually running automobiles, Proc. Inter-noise 92, pp.849-852, 1992
7) Y.Hidaka and H.Tachibana : Measurement of sound radiation from Shinkansen train by sound intensity method, Proc. Inter-noise 95, pp.215-218, 1995
8) H.Tachibana : Visualization of sound fields by sound intensity technique, Proc. of the 2nd Symposium on Acoustic Intensity, pp.117-126, 1988
9) S.Ise, H.Yano and H.Tachibana : Basic study on active noise barrier, J. Acoust. Soc. Jpn.(E), Vol.12 No.6, pp.299-306, 1991
10) S.Sakamoto, S.Ise and H.Tachibana : Experiment and FEM analysis of active noise control applied to a multiple chamber duct system, Proc. Inter-noise 94, pp.1397-1400, 1994
11) Y.Hidaka, H.Yano and H.Tachibana : Analysis of room acoustics by introducing 3D sound intensity measurement, Proc.of Acoust. Soc. Jpn Autumn Meeting, pp.793-794, 1993
12) H.Yano and H.Tachibana : Applications of sound intensity technique to architectural intensity measurement, J. Acoust. Soc. Jpn.(J), Vol.43 No.12, pp.966-974, 1987

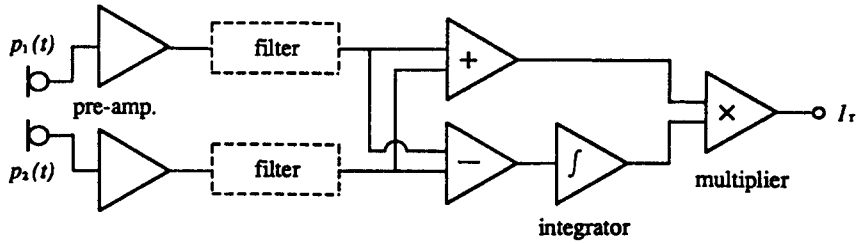

(a) Direct method

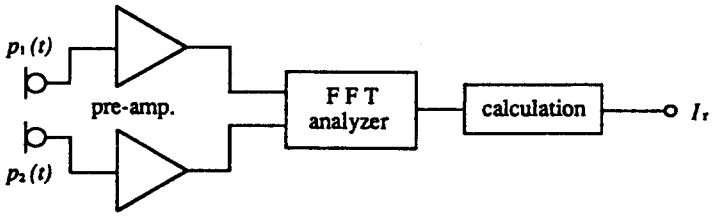

(b) Cross-spectrum (FFT) method

Fig.1 Sound intensity measurement systems by 2-mic. method

(a) side by side (b) face to face

Fig.2 2-microphone intensity probes

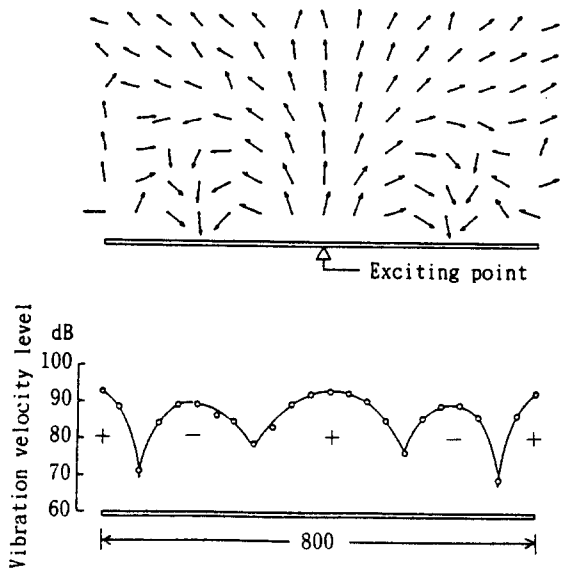

Fig.3 Sound radiation from a vibrating plate

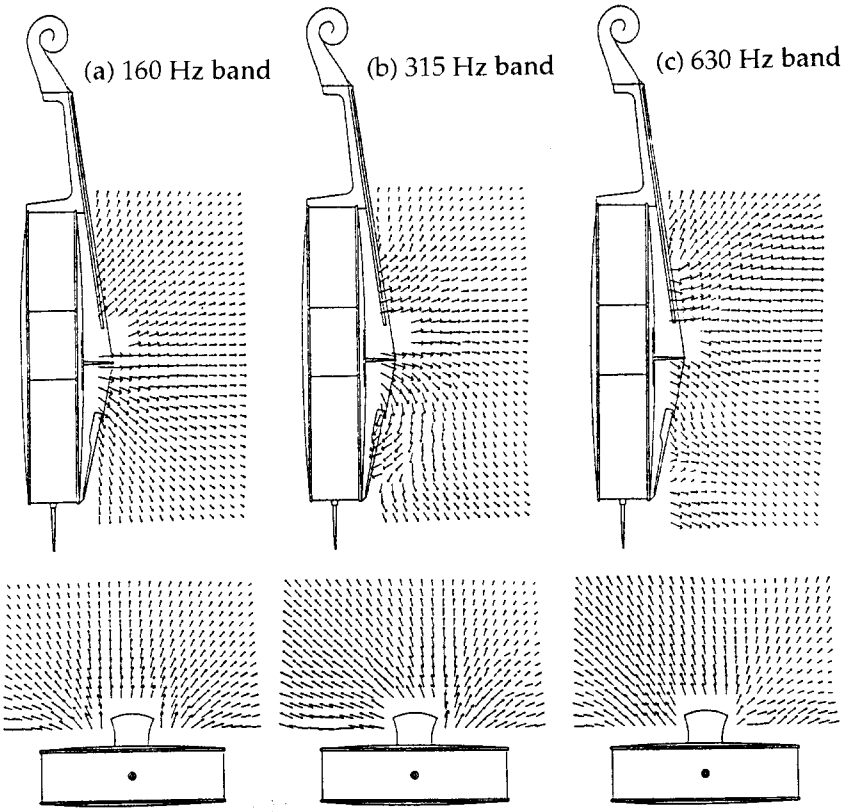

Fig.4 Measurement of sound power flow from a violoncello
Sound intensity vector map on the planes perpendicular to the sound board (1/3 octave band)

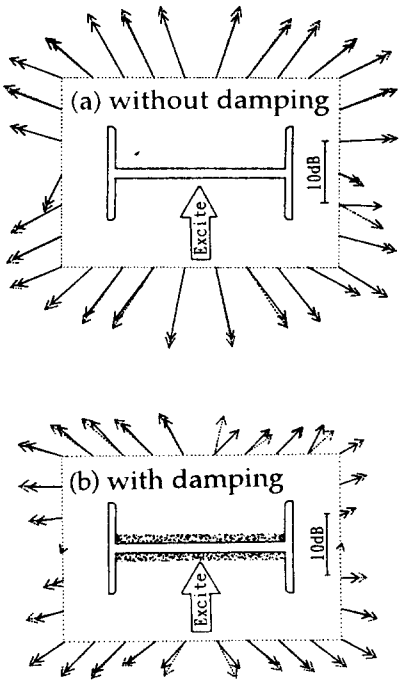

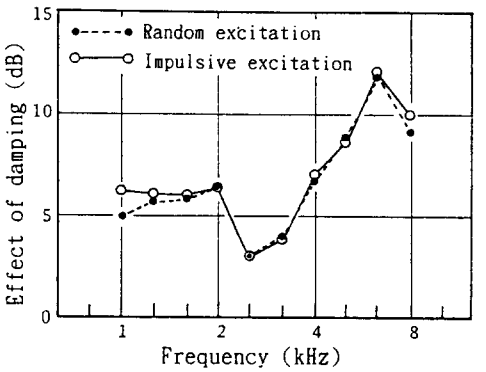

Fig.6 The effect of the damping treatment

Fig.5 Sound radiation from I-shaped steel beam
(4 kHz in 1/3 octave band)

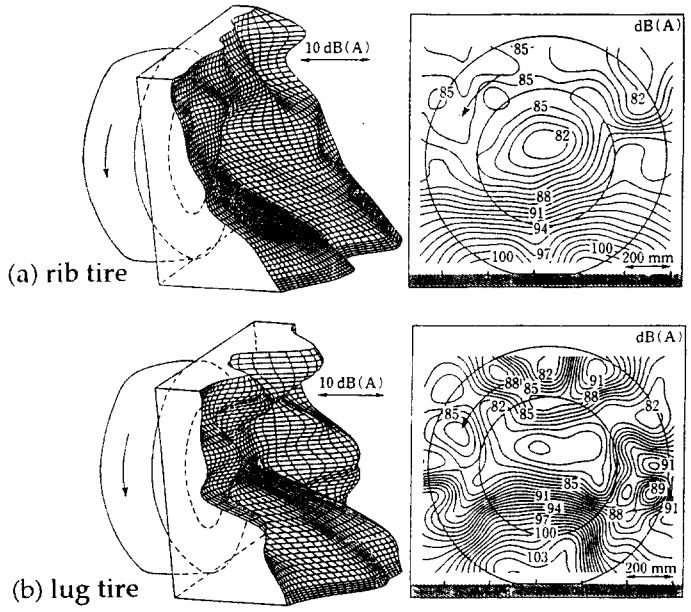

Fig.7 Sound intensity radiation from rolling tires (A-weighted)

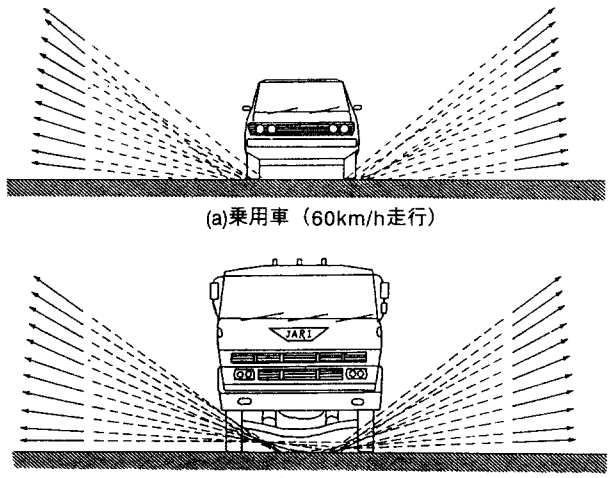

Fig.8 Sound intensity radiation from running automobiles (A-weighted)

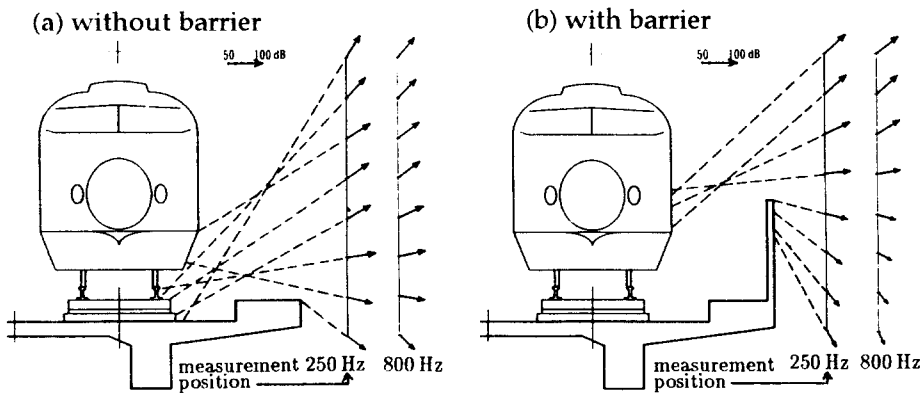

Fig.9 Sound intensity radiation from a Shinkansen train (233 km/h, 250 Hz: 1/3 oct. band)

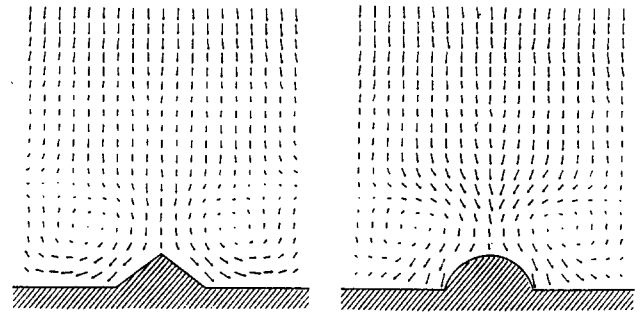

(a) 500 Hz

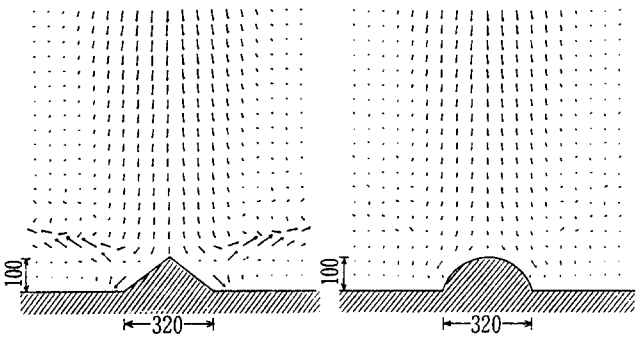

(b) 8 kHz

Fig.10 Sound reflection by planes with different projections

(a) ANC : OFF

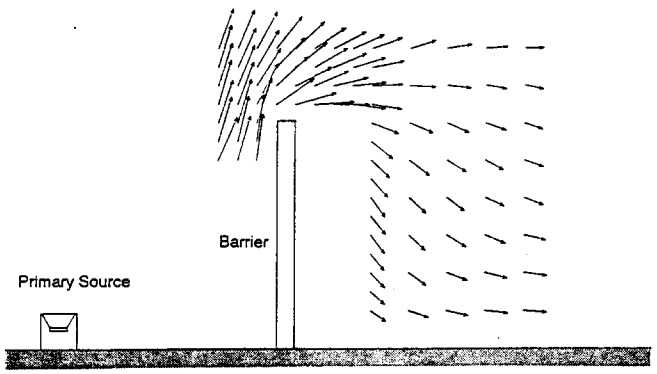

(b) ANC : ON

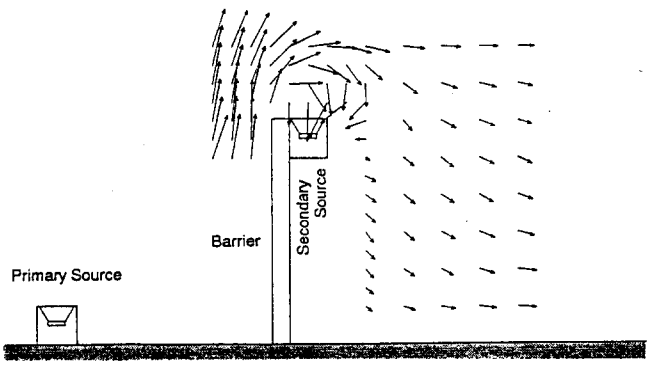

Fig.11 Sound intensity flow over an active barrier

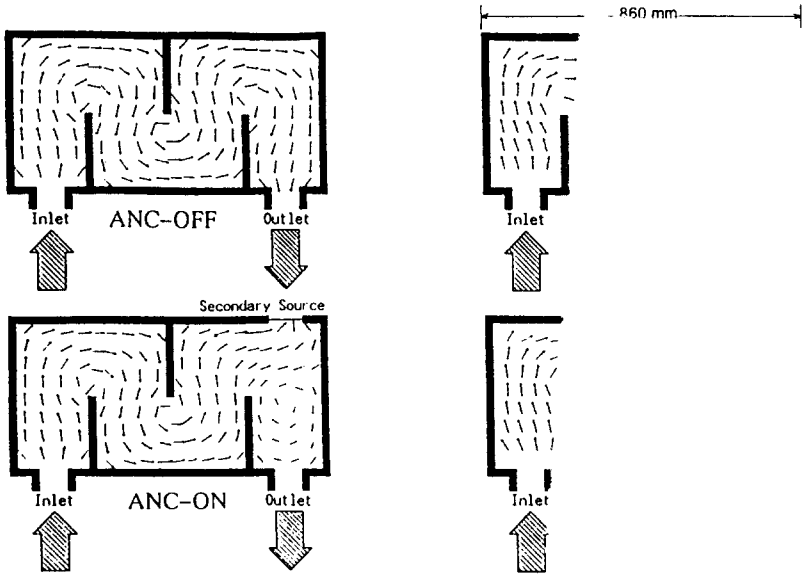

(a) FEM calculation results (b) e

Fig.12 Sound intensity flow in a maze-ty

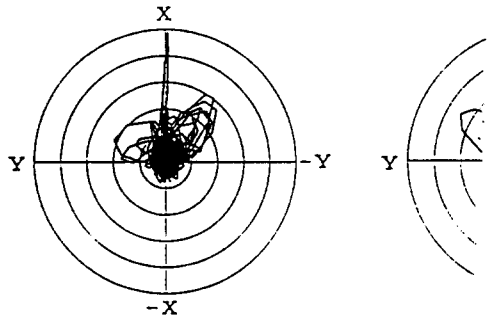

(a) concert hall (b) re

Fig.13 Vector loci of instantaneous sound in

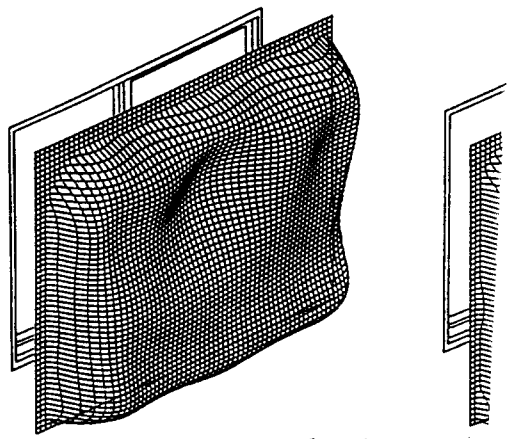

(a) 250 Hz in octave band

Fig.14 Sound intensity transmit